

## Aperture effects in Kirchhoff migration

T. Hertweck, C. Jäger, A. Goertz, and J. Schleicher

**email:** [Thomas.Hertweck@gpi.uni-karlsruhe.de](mailto:Thomas.Hertweck@gpi.uni-karlsruhe.de)

**keywords:** Kirchhoff migration, aperture, Method of Stationary Phase

### ABSTRACT

*Seismic images obtained by Kirchhoff time or depth migration are always accompanied by some artifacts known as “migration noise”, “migration boundary effects”, or “diffraction smiles”, which may severely affect the quality of the migration result. Most of these undesirable effects are caused by a limited aperture if the algorithms make no special disposition to avoid them. Likewise, strong amplitude variation along reflection events may also cause similar artifacts. All these effects can be explained mathematically by means of the Method of Stationary Phase. However, such a purely theoretical explication is not always easy to understand for applied geophysicists. By relating the terms of the stationary-phase approximation to simple geometrical situations, a more physical interpretation of the migration artifacts can be obtained. A simple numerical experiment for poststack (zero-offset) data indicates the problem and helps to develop an intuitive understanding of the effects and the methods to avoid them.*

### INTRODUCTION

Since the early work of Hagedoorn (1954), migration concepts have strongly improved and are now an important tool in the world of seismic imaging, either as prestack or poststack time and depth migration. A frequently used method is Kirchhoff migration (Schneider, 1978) that treats each depth point  $M$  on a sufficiently dense grid like a diffraction point. In an a-priori given macrovelocity model, the relevant part of the Green’s function of a point source at any single diffraction point  $M$  in the depth domain is calculated. The kinematic part of this Green’s function is the configuration-specific diffraction-traveltime surface, also called “Huygens surface”. The amplitudes of the input seismograms (or, to be more specific, of their derivatives) are stacked along the Huygens surface and assigned to the depth point  $M$ . This explains why the Kirchhoff migration scheme is also called a “diffraction stack”. If so desired, the effect of geometrical spreading can be removed from the output amplitudes by multiplying the data during the stack with a true-amplitude weight factor that is calculated from the dynamic part of the Green’s function.

Ideally, the extent of the Huygens surfaces, that is, the migration aperture, should be limitless so that no contributions due to the abrupt truncation of the sum occur. In practice, of course, the aperture is always limited by the region over which seismic data have been acquired. In other words, because of the finiteness of the survey area, Kirchhoff migration will always be a “limited aperture migration” (LAM) (Sun, 1998). This is, however, not the only reason why we have to deal with the effects of a finite migration aperture. In practical migration implementations, even ranges of source and receiver positions might be excluded where data actually have been acquired. Such a procedure can be advantageous because

- less traces to sum leads to a speedup of the whole migration process,
- a smaller operator excludes steeper dips, which helps to avoid operator aliasing (see, e.g., Abma et al., 1999),
- less summation of data away from the signal reduces the stacking of unwanted noise.

For the best possible reduction of aliasing and noise as well as the best computational efficiency, one would like to use a model-based aperture restriction, i.e., one would like to make use of the (projected) Fresnel zone (see, e.g., Schleicher et al., 1997; Sun and Bancroft, 2001). Unfortunately, it is difficult to determine the exact center and size of the Fresnel zone for each depth point prior to or during migration. A reasonable compromise between accuracy and practicability is to specify a common maximum migration aperture radius or a maximum stacking operator dip. These aperture reductions lead to dip-restricted migration operators as, for example, a 45° migration. With these kinds of operators, higher dips cannot be imaged. In regions where dips are known to be restricted, this is a very convenient way of reducing aliasing and improving computational efficiency at the same time. It should, however, be kept in mind that close to the maximum dip, these dip-restricted migration operators will achieve only kinematically correct images (see, e.g., Schleicher et al., 1997; Sun, 1998). For true-amplitude migration, the maximum operator dip must always be chosen somewhat larger than the maximum reflector dip to be imaged.

The fact that the migration aperture is limited causes artifacts known as migration noise, boundary or aperture effects, or migration smiles. In this paper, we relate the mathematical explanation of the migration artifacts by means of the Method of Stationary Phase (see, e.g., Bleistein, 1984; Sun, 1998; Bleistein et al., 2001) to simple geometrical situations. This more physical interpretation leads to a more intuitive insight into these effects. Of course, since the stacking operations are the same in Kirchhoff time and depth migration, the corresponding artifacts are conceptually identical in both processes. Thus, we restrict our present discussion to Kirchhoff depth migration. It should, however, be kept in mind that everything said and shown in this paper with respect to an image in depth holds in the same way for an image in time.

### KIRCHHOFF MIGRATION

Mathematically, the Kirchhoff migration process is expressed as an integration over the recorded wavefield and reads in 3D (Tygel et al., 1996)

$$V(M) = -\frac{1}{2\pi} \iint_A d\xi_1 d\xi_2 W_{DS}(\vec{\xi}, M) \left. \frac{\partial U(\vec{\xi}, t)}{\partial t} \right|_{t=\tau_D(\vec{\xi}, M)}, \quad (1)$$

where  $V(M)$  is the value assigned to one diffraction point  $M$  in the depth domain after migration and  $U(\vec{\xi}, t)$  denotes the data in the time domain (seismograms). These data are assumed to consist of analytic traces which allows the handling of complex reflection coefficients (supercritical reflections) and possible caustics along the ray paths. An analytic trace is formed by the actual trace recorded in the field as the real part and its Hilbert transform as the imaginary part. The vector  $\vec{\xi} = (\xi_1, \xi_2)$  is the so-called configuration parameter vector and represents the trace position. Sources and receivers are grouped into pairs, whose locations are described as a function of  $\vec{\xi}$ . The actual form of this function depends on the measurement configuration. The migration aperture  $A$  is the area over which  $\vec{\xi}$  varies to cover all source-receiver pairs used in the stack.

The factor  $W_{DS}(\vec{\xi}, M)$  is a true-amplitude weight function which may (true-amplitude migration) or may not (purely kinematic migration) be included in the migration scheme. The stacking surface  $\tau_D(\vec{\xi}, M)$  is the above-mentioned Huygens surface. The time derivative is needed in order to correctly recover the source pulse (Newman, 1975).

We assume that at least one reflection event is present in the seismic data  $U(\vec{\xi}, t)$ . Then, these data can be described by zero-order ray theory (see, e.g., Červený, 2001) as

$$U(\vec{\xi}, t) = R_c \frac{\mathcal{B}}{\mathcal{L}} \cdot F(t - \tau_R), \quad (2)$$

where  $R_c$  denotes the angle-dependent reflectivity,  $\mathcal{L}$  symbolizes the point-source geometrical spreading factor, and  $\mathcal{B}$  describes all other effects on the amplitude, such as source strength, source and receiver coupling, transmission loss and attenuation in the reflector overburden, to name a few. Moreover,  $F(t)$  is the analytic source wavelet which is shifted to the arrival time  $\tau_R$  (reflection traveltimes). A seismic trace with several (primary) events may be described by superposition of individual seismic events of the type of equation (2).

To enable a Fourier transform, we introduce the time  $t$  as an additional parameter in equation (1). This is nothing but a mathematical trick that can be undone by setting  $t = 0$ . Then, we can rewrite equation (1) in the frequency domain as

$$\hat{V}(M, \omega) = -\frac{i\omega}{2\pi} \hat{F}(\omega) \iint_A d\xi_1 d\xi_2 W_{DS}(\vec{\xi}, M) R_c \frac{\mathcal{B}}{\mathcal{L}} e^{i\omega\tau_{dif}}, \quad (3)$$

where  $\hat{F}(\omega)$  and  $\hat{V}(M, \omega)$  denote the Fourier transforms of  $F(t)$  and  $V(M, t)$ , respectively. Moreover,  $\tau_{dif}(\vec{\xi}, M)$  is the difference between the diffraction and reflection traveltimes, i.e.,  $\tau_{dif} = \tau_D - \tau_R$ .

In 2.5D, i.e., when the medium does not vary with respect to the coordinate perpendicular to the seismic line (crossline direction), the out-of-plane  $\xi_2$ -integration in equation (3) can be evaluated analytically. Since all data acquired on lines parallel to the actual seismic line would be identical, the migration aperture  $A$  can be assumed to be infinite in the  $\xi_2$ -direction. Kirchhoff migration then reduces to an in-plane stack over the aperture interval  $(a, b)$  in the  $\xi_1$ -direction covered by the seismic line. Since  $\xi_1$  is now the only integration variable, we can drop the index 1 to write the 2.5D Kirchhoff migration integral as

$$\hat{V}(M, \omega) = \sqrt{\frac{-i\omega}{2\pi}} \hat{F}(\omega) \int_a^b d\xi W_{DS}^{(2.5)}(\xi, M) R_c \frac{\mathcal{B}}{\mathcal{L}} e^{i\omega\tau_{dif}}, \quad (4)$$

where  $W_{DS}^{(2.5)}$  is the 2.5D weight factor that guarantees true amplitudes in this 1D stack. It is composed of the 3D weight factor and the result of the analytic solution of the out-of-plane integral.

### THE METHOD OF STATIONARY PHASE

In general, the integrals in equation (3) and the remaining integral in equation (4) cannot be solved analytically. The Method of Stationary Phase provides a way of analyzing their main contributions. Although in principle a high-frequency approximation, the Method of Stationary Phase yields highly accurate predictions of the migration results in the seismic frequency range. Mathematically, the prerequisites for applying the Method of Stationary Phase are implicitly fulfilled, since we perform all calculations within the framework of zero-order ray theory which is strictly valid only for high frequencies.

For simplicity, we restrict the following analysis to the 2.5D case. Conceptually, there is no difference in the application of the Method of Stationary Phase to the double integral for 3D migration. The qualitative discussion involves the same arguments and leads to the same conclusions. The quantitative analysis is similar but slightly more complicated, mainly resulting in a different amplitude behavior of the artifacts.

Reducing it to its basic structure, the integral in equation (4) can be written in the form

$$I(\omega) = \int_a^b f(\xi) e^{i\omega q(\xi)} d\xi . \quad (5)$$

The Method of Stationary Phase is based on the observation that for high frequencies, i.e., for large values of  $\omega$ , the factor  $e^{i\omega q(\xi)}$  oscillates very rapidly, thus covering full periods in very small intervals of  $\xi$ . If  $f(\xi)$  is not itself an oscillating function, its values do not strongly vary in any such interval. Thus, the integration over a full period of  $e^{i\omega q(\xi)}$  yields approximately zero and does not contribute to the overall value of the integral. The only regions where  $e^{i\omega q(\xi)}$  does not oscillate are those where the phase function  $q(\xi)$  remains approximately constant or *stationary*. Mathematically, points of stationary phase are those where the phase function  $q(\xi)$  has a horizontal tangent, i.e., a vanishing derivative. Non-negligible contributions to integral (5) are, therefore, to be expected from the vicinity of these points. Further contributions to integral (5) are to be expected from the boundaries of the integration interval because there, the integration generally does not cover a full period of  $e^{i\omega q(\xi)}$ .

To illustrate the above observations, we consider the migration of zero-offset data from a simple earth model with a horizontal reflector at a depth of 1 km. For a point  $M$  at  $x = 3$  km on the reflector and a frequency of 30 Hz, Figure 1(a) and (b) show the phase and amplitude (dashed line) of the integrand in equation (4), respectively, as a function of  $\xi$ . Part (b) also shows the real part of the full integrand function. Note that this function strongly oscillates everywhere except in the vicinity of the point where the phase is stationary. It is evident that the amplitude modulation does not alter the oscillatory character of the integrand function (if the above mentioned assumptions for  $f(\xi)$  are fulfilled).

Let us now discuss integral (5) in a more quantitative way. In our case, the phase function  $q$

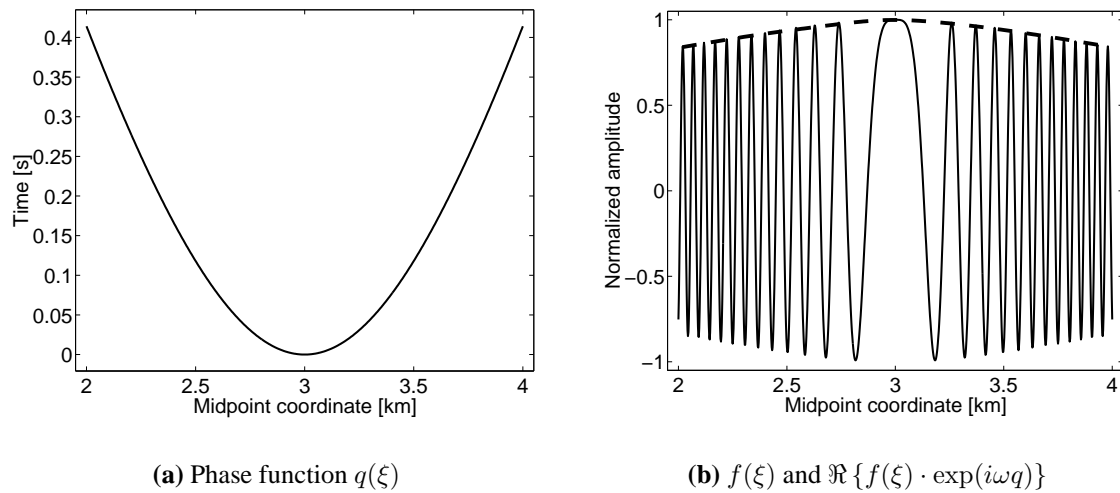


**Figure 1:** Illustration of the integrand in equation (4). (a) Phase function  $q(\xi)$ . (b) Amplitude function  $f(\xi)$  (dashed line) and real part of the complete integrand function  $f(\xi) \cdot \exp(i\omega q)$  (solid line).

is the difference between the diffraction and reflection traveltime curves,  $\tau_{dif}$ . Thus, the real part of the integrand function (Figure 1(b)) has zeroes at

$$|\tau_{dif}| = |\tau_D - \tau_R| = n \frac{\pi}{\omega} = n \frac{T}{2}, \quad (6)$$

where  $T = 2\pi/\omega$  is the period of the monofrequency wave under consideration. Equation (6) is equivalent to the definition of the boundary of the  $n$ th Fresnel zone (see, e.g., Červený and Soares, 1992). Therefore, the alternating zones of negative and positive amplitude of the integrand function are physically equivalent to the Fresnel zones<sup>1</sup>.

Now, consider an integration of the function  $f \cdot \exp(i\omega q)$  from the center (where  $\tau_D = \tau_R$ ) to the sides. At first, this sums up positive contributions from the first Fresnel zone, ending at the first zero in either direction. Subsequent Fresnel zones, each ending at the next zero, will add purely negative or positive contributions to integral (5). In other words, Fresnel zones with odd numbers contribute positively to the integral while Fresnel zones with even numbers contribute negatively. Because of the above observation that an integration over a full period, i.e., over two consecutive Fresnel zones, yields approximately zero, it becomes clear why the principal contribution to integral (5) will stem from the vicinity of the stationary point. Hence, an integration over only the first Fresnel zone already provides a very good approximation of the total integral. On the other hand, its full value cannot be recovered, if the integration interval does not cover the first Fresnel zone completely.

<sup>1</sup>To be exact, what is involved in Kirchhoff migration is the projected Fresnel zone in the data space (Hubral et al., 1993). The true Fresnel zone in depth can be observed in the Kirchhoff modeling integral. Conceptually, however, there is no difference.

It has to be noted, however, that the above discussion holds strictly only for a monofrequency signal. For a transient, band-limited signal, one has to replace the half-period  $T/2$  in equation (6) by some estimate of the wavelet length  $\tau_W$ .

An analysis of the migration integral (5) by means of the Method of Stationary Phase under the assumption of a single, simple and isolated point of stationary phase yields, up to second order in  $1/\sqrt{\omega}$ ,

$$I(\omega) \simeq f(\xi^*)e^{i\omega q(\xi^*)} \sqrt{\frac{2\pi}{-i\omega q''(\xi^*)}} + \frac{1}{i\omega} \left[ \frac{f(b)}{\frac{dq}{d\xi}\Big|_b} e^{i\omega q(b)} - \frac{f(a)}{\frac{dq}{d\xi}\Big|_a} e^{i\omega q(a)} \right]. \quad (7)$$

For high frequencies, these expressions describe the major contributions to the final migrated image. The first term stems from the stationary point  $\xi^*$  of the phase  $q = \tau_D - \tau_R$ , that is, the tangency point between the Huygens and reflection traveltimes curves, and forms the actual migrated image of the reflector(s). In general, this contribution will be the dominant part of the total migrated section. The second term comes from the endpoints of the integration/stacking operator. It is this second contribution that describes the main migration artifacts. Because of the higher order in  $1/\sqrt{\omega}$ , its amplitudes generally will be lower than those of the reflector image. Note, however, that under certain circumstances these effects can be as strong as (or even stronger than) a reflector image.

It is to be remarked that migration artifacts due to a limited aperture, illumination problems, or missing traces are inherent to seismic migration, independently of the actual migration scheme employed. Artifacts due to strong amplitude variations and focusing effects are, however, a consequence of Kirchhoff migration and can be largely reduced with other migration schemes such as, e.g., finite-difference wave-equation migration.

In contrast to the data boundaries, actually ending reflectors in the earth do not provoke migration smiles. In this case, edge diffractions are present in the seismic data that are collapsed by migration into the endpoint of the reflector. Because of the diffractions, the reflection event in the data has no actual endpoint but dies off over a larger number of traces. In this way, endpoint contributions are suppressed. The latter observation already points towards a well-known way of suppressing migration artifacts: tapering. We will discuss this in a later section.

## GEOMETRICAL EXPLANATION OF THE APERTURE EFFECTS

The migration aperture effects are most easily explained by means of a simple numerical experiment for poststack data. The model consists of two half-spaces separated by a horizontal interface. The velocities in the upper and lower half-spaces are  $v_p^{(1)} = 2$  km/s and  $v_p^{(2)} = 3$  km/s, respectively, and the shear wave velocities are given by  $v_s = v_p/\sqrt{3}$ . The density is constant in the whole model. The zero-offset seismogram was generated by dynamic ray tracing using a zero-phase Ricker wavelet with 20 Hz, a time sampling of  $dt = 1$  ms and a trace distance of  $\Delta\xi = 5$  m. It was migrated with a 2.5D Kirchhoff true-amplitude depth migration scheme on a dense grid ( $dx = 10$  m,  $dz = 2$  m) using the true velocity.

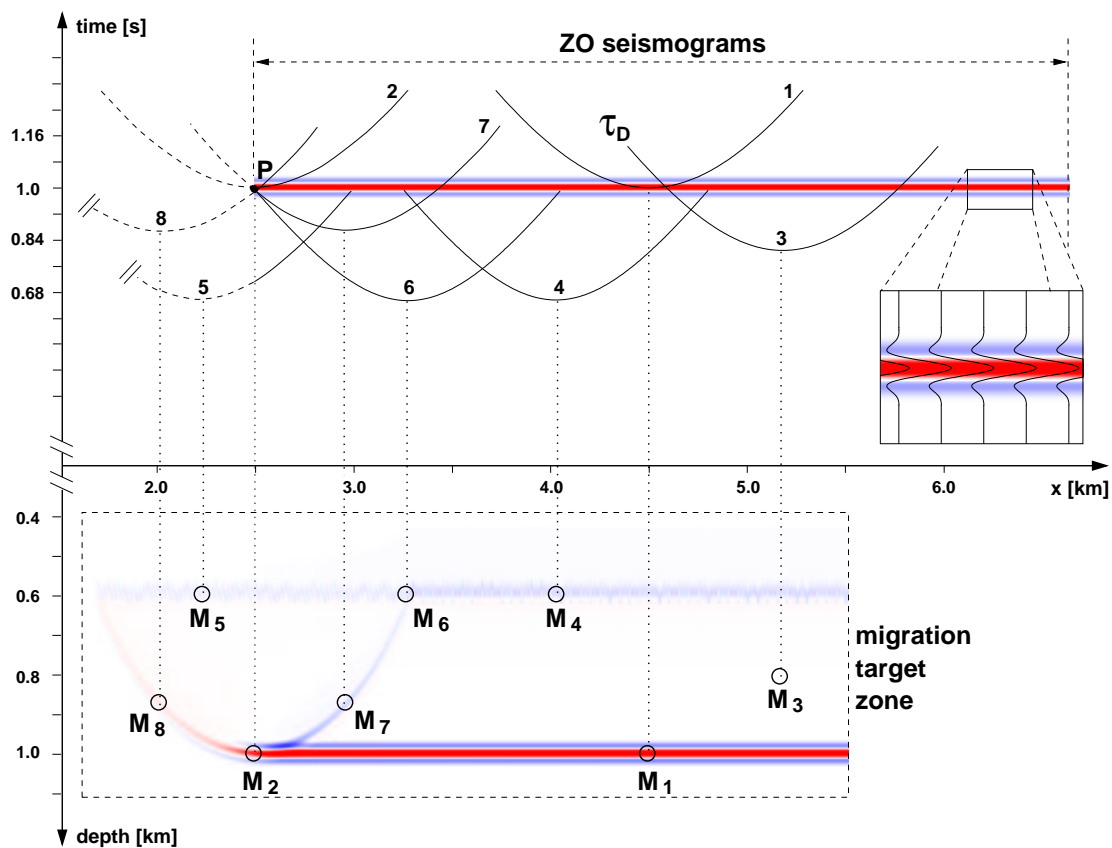


**Figure 2:** ZO seismogram and corresponding depth image after poststack migration. Several characteristic depth points  $M_j$  and their pertinent stacking operators are shown. These are used to give a simple geometrical explanation of the limited aperture migration effects.

For this simple model, the stacking operator is given by a hyperbola. We limited its spatial extent to 800 m with respect to the horizontal coordinate of the apex. In this way, the number of traces contributing to the stack for each depth point was 320. The migration target zone was placed at the end of the survey line so as to show the boundary effects. The resulting migrated image is depicted in Figure 2. Note that no effort was made to enhance or reduce the migration artifacts.

By means of Figure 2, we are now going to discuss the boundary effects from a geometrical point of view, which allows us to gain a more intuitive insight. We then relate them to the above discussion of the interference in integral (5) and to the result of its stationary-phase evaluation as given by equation (7). For this purpose, we discuss the position of the Huygens curves pertaining to a series of characteristic depth points  $M_1$  to  $M_8$ .

### Points on the reflector: $M_1$

The actual reflector (which is unknown prior to migration) is built up by depth points like  $M_1$ . The pertinent Huygens curve is tangent to the reflection traveltime curve. Thus, amplitudes gath-

ered along such a curve sum up coherently and provide high stacking results that are assigned to the corresponding depth point. Note that in general, for laterally inhomogeneous media, the tangency point does not coincide with the apex of the stacking curve. To relate this physical explanation to our earlier considerations of the Method of Stationary Phase, we identify these tangency points with the “points of stationary phase”. The value assigned to  $M_1$  is mathematically described by the first term in equation (7). No boundary effects are present because the input data at the endpoints of the stacking operator, which correspond to the limits of integration  $a$  and  $b$  in equation (4), are zero. Of course, in practice there will always be some endpoint contributions because of the noise inherent in the seismograms.

### **Points on the reflector boundary: $M_2$**

The point  $M_2$  represents the boundary of the migrated reflector image. The Huygens curve of this point is, in principle, equivalent to the one of point  $M_1$ . However, since the stationary point is located directly at the margin of the ZO gather, only half the operator is within the data volume. Thus, summing up along the stacking curve results in an amplitude value which is half of the value assigned to  $M_1$ . This coincides with the stationary-phase analysis for the case when the stationary point falls on the boundary of the integration interval.

### **Points off the reflector: $M_3$**

Points like  $M_3$  represent the majority of diffraction points within the target zone. They have Huygens curves which completely cross the reflection signal. Summing up amplitudes along such operators leads to low values due to destructive interference. From a mathematical point of view, the point of stationary phase (i.e., where the traveltimes and Huygens curves have the same time dip) as well as the endpoints of the operator are outside the signal. Therefore, both terms in equation (7) are zero.

### **Migration artifacts caused by the finite stacking operator: $M_4$ , $M_5$ , and $M_6$**

For points like  $M_4$ , the endpoints of the stacking operator lie within the reflection signal. Because of the limited aperture, the stack does not sum up all the data necessary for complete destructive interference in the same way as it does for point  $M_3$ . Thus, the migration output at  $M_4$  is not as low as that for point  $M_3$ . In consequence, a migration artifact appears in parallel to the actual reflector. With increasing size of aperture, the effect at  $M_4$  moves away from the actual reflector and might be located outside of the target zone. Sun (1998) showed that this aperture effect completely separates from the reflector image if the aperture is larger than one Fresnel zone (see also Section “How to avoid aperture effects”).

The relationship of the above observations to the Method of Stationary Phase is straightforward. Like for point  $M_3$ , the point of stationary phase is outside the signal. However, the endpoints of the operator lie inside the signal. Therefore, the first term of equation (7) yields no contribution, but its second term predicts a non-zero migration output at  $M_4$ .



The situation at point  $M_5$  is in principle equivalent to that at point  $M_4$ . However, as only one endpoint lies within the reflection signal (the other endpoint lies outside the data), the amplitude at  $M_5$  is just half of that at  $M_4$ .

Point  $M_6$  marks the transition between the two situations of points  $M_4$  and  $M_5$ . The endpoint of its pertinent Huygens curve coincides with the boundary point  $P$  in the data, where the survey ends. It is for this reason that at  $M_6$  the migration artifact splits into two effects. Additionally to the limited-operator effect described above, a limited-data effect appears in the migrated traces.

### Migration artifacts caused by the finite survey area: $M_7$ and $M_8$

The most prominent migration artifact is the “migration smile” represented by points  $M_7$  and  $M_8$ . The pertinent Huygens curves cross the reflection signal exactly at the end of the survey line. In this way, the destructive interference is incomplete at one of the endpoints, thus leading to a non-negligible contribution.

It is worthwhile to observe that the position of the migration smile is given by the geometrical location of all points of the type of  $M_7$  and  $M_8$  whose Huygens curves cut the border point  $P$  of the reflection signal. Note that, because of the duality between the Huygens curve and the isochron (see, e.g., Tygel et al., 1995), this is the isochron of  $P$ . The resulting migration artifact follows this isochron, which is a half-circle for our constant-velocity zero-offset experiment as shown on the left side of Figure 3.

Observe the inverted polarity of the artifact between points  $M_7$  and  $M_8$ . This can be explained with the help of the symmetry of the operator. The dashed part of the Huygens curve of  $M_7$  that is outside the data is identical to the solid part of the Huygens curve of  $M_8$  that is inside the data. Thus, the stack at  $M_8$  will contribute with exactly that part of the data that is missing at  $M_7$ . The actual values of the migration results at points  $M_7$  and  $M_8$  depend on the form of the source wavelet as well as on the (half-)derivative applied in the migration process. However, the fact that these values are complementary to each other is independent of these conditions. For a better visualization of this complementarity, we have picked the peak amplitudes along both branches of the migration smile corresponding to points  $M_7$  and  $M_8$ . When adding the amplitude of two opposite points from the two branches, we can verify in Figure 3 (right side) that the sum at  $M_7$  and  $M_8$  indeed yields zero (except, of course, for a numerical error).

Again, we can directly relate the above physical interpretation to the terms of the stationary-phase evaluation of the Kirchhoff-migration integral. Of course, the migration outputs at points  $M_7$  and  $M_8$  are described by the second term in equation (7). The first term yields a zero contribution since the stationary point is outside the reflection signal as in the case of points  $M_3$ ,  $M_4$ ,  $M_5$ , and  $M_6$ . At both points,  $M_7$  and  $M_8$ , the actual contribution stems from the lower integral limit,  $a = 2500$  m. Since the Huygens curves of both points terminate at the same position,  $f(a)$  is the same for both of them. So where is the inverted polarity? It's in the sign of the derivative, i.e., in our simple example the dip of the stacking curve, at the survey end. As we can easily observe in Figure 2 this sign is positive for  $M_8$  but negative for  $M_7$ .

The Method of Stationary Phase evaluation allows for a more quantitative analysis of the migration smile. Using equation (7) and recalling the additional factor  $\sqrt{\omega}$  in front of the integral in equation (4) (which stems from the time half-derivative in the original Kirchhoff migration

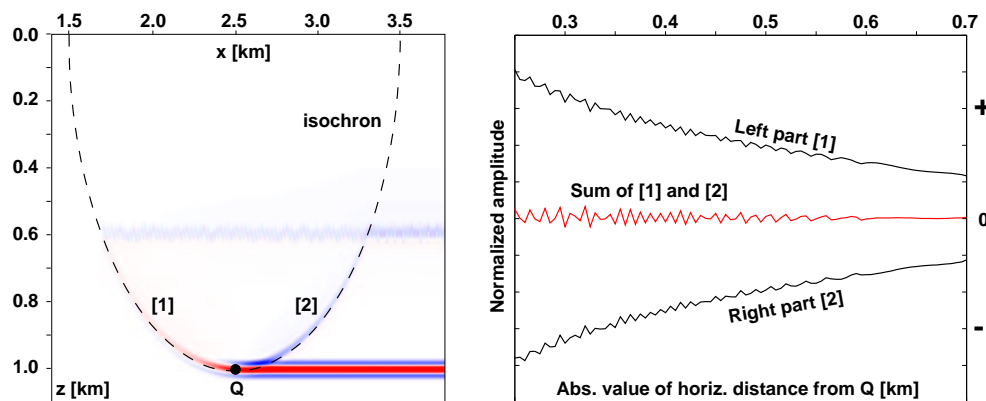


**Figure 3:** Analysis of the migration smile. Left side: Kinematically, it coincides with the isochron of the border point  $P$  of the data. Right side: The sum of peak amplitudes of two opposite points on the isochron branches [1] and [2] yields approximately zero.

integral), we see that the main contribution to the migration result will be frequency independent while the boundary effects will decay proportionally to  $1/\sqrt{\omega}$ . Figure I shows the amplitude of the migration output at points  $M_4$  (circles) and  $M_7$  (crosses) as a function of the dominant frequency of the source wavelet used in the modeling. The actually observed amplitudes follow almost exactly the predicted behavior (solid line).

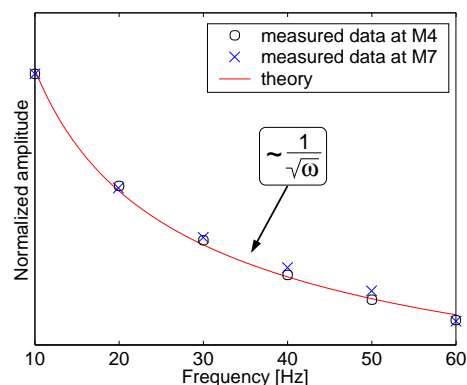


**Figure 4:** Frequency behavior of the boundary effects in 2.5D. The amplitude at  $M_4$  (circles) and  $M_7$  (crosses) decays with  $1/\sqrt{\omega}$  as predicted by the Method of Stationary Phase.

### HOW TO AVOID APERTURE EFFECTS

Above, we have already indicated that there is a well-known technique to reduce migration artifacts resulting from the limited migration aperture. All that has to be done is to avoid an abrupt end of the operator but let it die off over a couple of traces, i.e., apply a taper. This has to be done at two different places: Firstly, the input seismograms are tapered at the endpoints of the survey area. Secondly, the finite operator is not just truncated but also tapered at its endpoints. In terms

of the stationary-phase solution (7), the values of  $f(a)$  and  $f(b)$  are artificially set to zero. This has to be done smoothly in order not to violate the underlying assumption of a slowly varying function  $f(\xi)$ . Then, this approach reduces the contributions of the operator endpoints and, thus, helps to obtain a migrated image with less migration artifacts.

When applying a taper, the fundamental question is over how many traces it should extend. On the one hand, the taper ought to be large enough not to violate the smoothness assumption so as to effectively suppress the artifacts. On the other hand, it should not be too large so as not to lose more information than necessary on the amplitudes at the survey ends or to stack unnecessary information at the operator ends. Sun (1998) suggests that in the same way as the stacking region should cover the first (projected) Fresnel zone, the taper region should extend over the second (projected) Fresnel zone around the stationary point. Unfortunately, this point cannot be estimated prior to or during migration. Therefore, we have to use once again a compromise to avoid the aperture effects.

To get an idea about the size of the taper region, we propose the following simple criterion for zero-offset (poststack) migration. As is well-known, to kinematically migrate all reflectors at depth  $z$  up to maximum dip angle  $\theta_m$ , the stacking operator may be restricted to a radius of  $r = z \tan \theta_m$ . If the same reflectors are to be migrated dynamically correctly, the radius must be increased by the size  $FZ(1)$  of the projected first Fresnel zone, given in the frequency domain by

$$FZ(n) = \frac{\sqrt{\frac{vznT}{2 \cos \theta_m} + \left(\frac{nvT}{4}\right)^2}}{\cos \theta_m} \quad (8)$$

with  $n = 1$ , where  $v$  is the medium velocity and  $T$  the period of the considered monofrequency wave. Like in equation (6), the half-period  $T/2$  has to be replaced by some estimate of the wavelet length  $\tau_w$ , if formula (8) is to be applied in the time domain. According to Sun (1998), the artifacts are suppressed as well as possible, while affecting the amplitudes as little as possible, when the operator is increased by  $FZ(2)$  instead of  $FZ(1)$ . The additional operator extension  $FZ(2) - FZ(1)$  is the second projected Fresnel zone, over which the taper is to be applied. Of course, the formulas given above are strictly valid for constant velocity only. For inhomogeneous media, they can only be used as a “rule of thumb” to get a rough idea about the aperture size and the taper region.

Formula (8) can also be used to obtain an estimate for the size of the end-of-survey taper. By substituting  $z = vt \cos \theta_m / 2$  and setting  $n = 1$ , the size of the taper at two-way time  $t$  can be estimated. If a constant taper size is preferred,  $t$  can be replaced by the maximum time value in the data. Correspondingly,  $z$  in equation (8) can also be replaced by the maximum depth in the desired migrated image.

Figure 5 demonstrates the effect of tapering the input data and the stacking operator for different aperture and taper sizes. Figure 5(a) shows the migrated reflector image when stacked with a dip-limited  $0^\circ$  migration operator using the optimal aperture of one projected Fresnel zone, without applying a taper. Both the migration artifacts due to the limited operator and survey area are present. As we can see, the optimal aperture guarantees the separation of the end effect from the reflector image, the amplitudes of which are also correct. Figure 5(b) shows the same migrated reflector image with the optimal taper applied. Both artifacts are almost completely eliminated. In Figure 5(c), we see the effect of a too small taper. Although both migration arti-

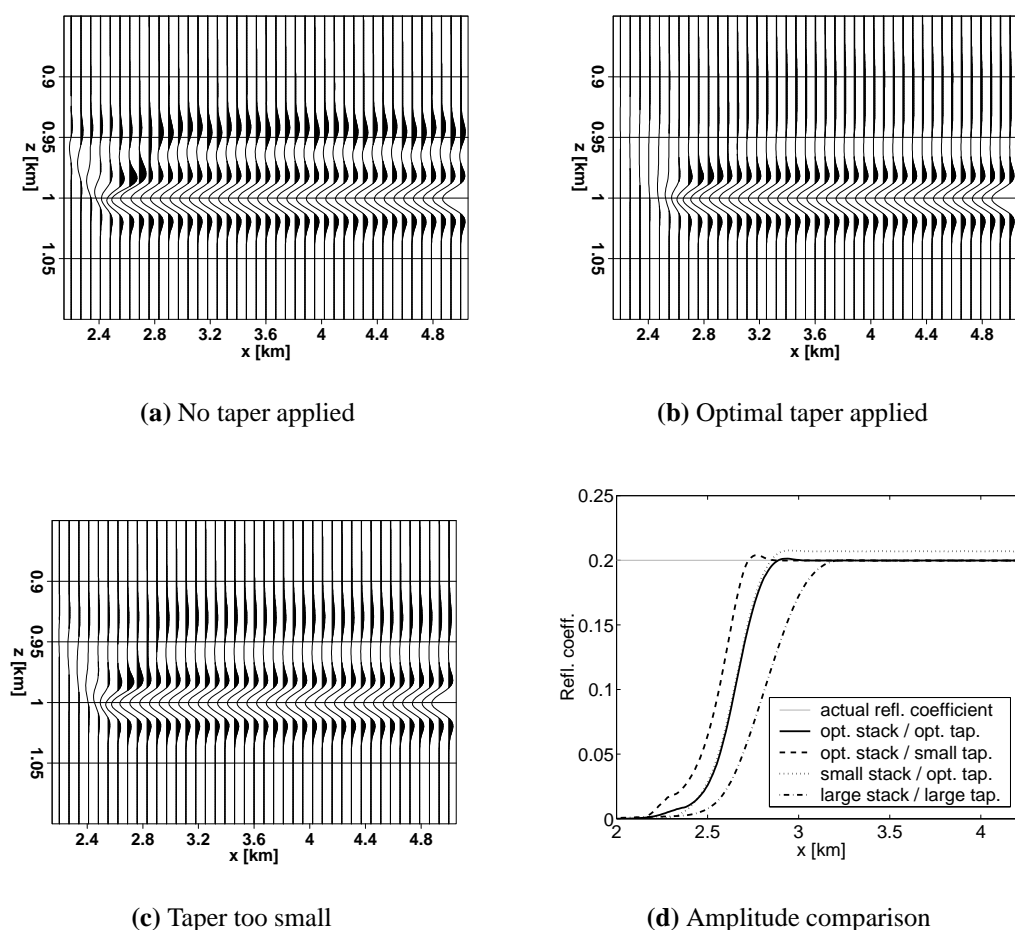


**Figure 5:** Effects of tapering. (a) Migration result without applying a taper function at all. (b) Migration result with taper function applied according to eq. (8). (c) Migration result with a taper function that is too small. (d) Amplitude comparison of different migration results with optimal and smaller/larger aperture/taper region, respectively.

facts are reduced, they remain clearly visible. Finally, Figure 5(d) compares the amplitudes along the reflector image for different combinations of aperture and taper sizes. When the aperture is too small, not even the amplitudes far away from the data margins are correctly recovered (dotted line), although the optimal taper is used. When the optimal (or a larger) aperture is applied, all amplitude problems are restricted to the data margins. For too small a taper, the survey-end artifact is not completely removed (dashed line). Too large a taper destroys the amplitudes where they can be retrieved from the data (dash-dotted line). The optimal taper size is the one that eliminates all artifacts but recovers the amplitudes as close to the margins as possible (solid line).

The taper function used for the migration examples shown here is a two-sided Hanning window for both the operator and the end-of-survey taper. For comparison, we also tested a two-

sided triangular window. The shapes of these functions are depicted in Sun (1998, 2000) for 2D and 3D. Both types of taper functions yield nearly identical results. The optimal values for the aperture and taper sizes were calculated by means of equation (8) with  $z = 1$  km,  $v = 2$  km/s,  $\tau_w = 50$  ms, and  $\theta_m = 0^\circ$ , resulting in  $FZ(1) = 320$  m and  $FZ(2) = 458$  m. To test the effect of a too small and large aperture or taper size, respectively, the stacking region  $FZ(1)$  and the taper region  $FZ(2) - FZ(1)$  were halved or doubled.

## CONCLUSION

Artifacts known in Kirchhoff migration as “migration noise”, “migration boundary effects” or “diffraction smiles” can be mathematically explained by means of the Method of Stationary Phase. In this paper, we have provided a more physical explanation of these effects by discussing the constructive and destructive interference of the stack in simple geometrical situations. This helps to relate the terms of the stationary-phase approximation with the actually observed migration artifacts. It turned out that, for practical applications, one has to distinguish between two principal types of artifacts. These are boundary effects due to a limited survey aperture, and artifacts due to a limited migration operator. Both types of artifacts are mathematically equivalent and can be explained by means of the boundary terms that result from the stationary-phase analysis of the migration integral. As predicted by the Method of Stationary Phase, the principal migration artifacts in 2.5D exhibit a  $1/\sqrt{\omega}$  decay as compared to the reflector image.

Based on our geometrical analysis, we had a closer look at a well-known way to avoid the aperture effects: tapering. The most important question with respect to tapering is how to determine the taper region. Too small a region won't suppress the effects while too large a region will destroy more information than necessary. We have shown that the ideal taper region is closely connected to the minimum aperture.

Schleicher et al. (1997) have derived the minimum aperture for a dynamically correct migration to be the first projected Fresnel zone (Hubral et al., 1993) around the specular point. Sun (1998) has demonstrated that the same minimum aperture of the size of the first projected Fresnel zone is sufficient to separate the operator-end effect from the desired image. We have confirmed both observations numerically. Moreover, to get rid of the operator-end effect, a taper region of the size of the second projected Fresnel zone should be added to the operator. In principle, the projected Fresnel zone(s) can be determined during migration, even in inhomogeneous media, from dynamic ray quantities. However, to speed up the process, it is often useful to fix the operator size beforehand. Then, the constant-velocity formula should help to get an idea of an adequate aperture and taper region.

## PUBLICATIONS

The mathematical derivations, some further explanations, and a comparison to Sun (2000) will be published in a forthcoming paper.

## ACKNOWLEDGMENTS

The authors thank Norman Bleistein for his careful reading and constructive criticism of the manuscript. This work was kindly supported in part by the Research Foundation of São Paulo (FAPESP), Brazil, the Brazilian National Research Council (CNPq), and the sponsors of the Wave Inversion Technology (WIT) Consortium, Karlsruhe, Germany.

## REFERENCES

- Abma, R., Sun, J., and Bernitsas (1999). Antialiasing methods in Kirchhoff migration. *Geophysics*, 64(6):1783–1792.
- Bleistein, N. (1984). *Mathematical methods for wave phenomena*. Academic Press Inc., Orlando.
- Bleistein, N., Cohen, J., and Stockwell, Jr., J. (2001). *Mathematics of Multidimensional Seismic Imaging, Migration, and Inversion*. Springer-Verlag Inc., New York.
- Červený, V. (2001). *Seismic Ray Theory*. Cambridge University Press, Cambridge.
- Červený, V. and Soares, J. (1992). Fresnel volume ray tracing. *Geophysics*, 57:902–915.
- Hagedoorn, J. (1954). A process of seismic reflection interpretation. *Geophys. Prosp.*, 2(2):85–127.
- Hubral, P., Schleicher, J., Tygel, M., and Hanitzsch, C. (1993). Determination of Fresnel zones from traveltimes measurements. *Geophysics*, 58(5):703–712.
- Newman, P. (1975). Amplitude and Phase Properties of a Digital Migration Process. In *Annual EAEG Meeting (Extended Abstracts)*. (Republished in: *First Break*, 8, 397–403, 1990).
- Schleicher, J., Hubral, P., Tygel, M., and Jaya, M. (1997). Minimum apertures and Fresnel zones in migration and demigration. *Geophysics*, 62(1):183–194.
- Schneider, W. (1978). Integral formulation for migration in two and three dimensions. *Geophysics*, 43(1):49–76.
- Sun, J. (1998). On the limited aperture migration in two dimensions. *Geophysics*, 63(3):984–994.
- Sun, J. (2000). Limited aperture migration. *Geophysics*, 65(2):584–595.
- Sun, S. and Bancroft, J. (2001). How much does the migration aperture actually contribute to the migration result? In *Annual SEG Meeting (Expanded Abstracts)*.
- Tygel, M., Schleicher, J., and Hubral, P. (1995). Dualities between reflectors and reflection-time surfaces. *J. Seis. Expl.*, 4(2):123–150.
- Tygel, M., Schleicher, J., and Hubral, P. (1996). A unified approach to 3-D seismic reflection imaging, Part II: Theory. *Geophysics*, 61(3):759–775.